Accuracy of an OTA System Emulating a Realistic 3D Environment for GNSS and Multi-Satellite Receiver Testing

Christopher Schirmer*§, Wim A. Th. Kotterman§, Gregor Siegert‡, Alexander Rügamer‡,
Giovanni Del Galdo*§‡, Albert Heuberger‡ Markus H. Landmann‡,
*International Graduate School on Mobile Communications (MobicoM)
§Institute of Information Technology, Ilmenau University of Technology,
Helmholtzplatz 2, 98684 Ilmenau, Germany
‡Fraunhofer Institute for Integrated Circuits IIS, 91058 Erlangen, Germany
Email: christopher.schirmer@tu-ilmenau.de

***Abstract*—In satellite-based systems, such as global navigation satellite systems (GNSS), the use of antenna arrays is becoming increasingly common, as it allows various applications, such as jammer/spoofer suppression or improving the positioning accuracy in multipath-environments. Testing such equipment under realistic and reproducible conditions is often not feasible, for example in the case of a not fully deployed system (e. g., Galileo satellites) or testing of classified transmission technologies (e. g., Galileo public regulated service (PRS) receivers). For tests under reproducible and realistic conditions, we propose 3D wave-field synthesis (WFS) in an over-the-air testbed. This allows a realistic emulation of the radio environment under laboratory conditions.**

In this paper, a feasibility study for such a testbed is presented. Possible antenna setups for a 3D WFS laboratory environment are proposed. For these setups, the 3D WFS accuracy is investigated for emulating different polarization types and multipath reflections with arbitrary source directions. The results show that with presently available hardware for channel emulation and 3D WFS, a virtual electromagnetic environment can be created for testing receivers with (beamforming) antenna arrays of typical size (120 mm–300 mm diameter).

***Index Terms*—anechoic chamber, GNSS, MIMO, over-the-air testing, polarization, signal processing, testing, wave-field synthesis**

I. Introduction

The use of multiple antennas in communication systems is paramount to achieve high data rates, as it gives access to the spatial dimension. Recently, antenna arrays have made their way also in global navigation satellite systems (GNSS) as they can be employed to suppress jammers and spoofers as well as to improve reception in multi-path environments.

The complexity of devices employing multiple antennas, however, requires the design of appropriate testing procedures, as it is mandatory to uncover possible functional problems while avoiding interference with other devices sharing the same spectrum. Traditionally, conducted tests are used to assess behavior of a radio device. To do so, the antenna of the device under test (DUT) is removed in order to connect it to the testing equipment via cables. However, in such a way, the antenna behavior cannot be included. To overcome this issue, several methods are proposed in [1]. The two-stage method, explained in [2], [1], was proposed. For the purpose of GNSS receiver testing the two stage method and the multiprobe OTA method seem to be appropriate to account for the antenna influence. Nevertheless, the two-stage method requires to detach the DUTs antenna, which is not always possible without damaging the DUT.

A solution for the mentioned problems is the over-the-air testing in a virtual electromagnetic environment (OTA*in*VEE, [3]), which is currently under construction at the Fraunhofer Institute for Integrated Circuits IIS at the facility for over-the air-research and testing (FORTE) in Ilmenau, Germany. For GNSS testing, following the OTA*in*VEE approach, we propose the testbed as shown in Figure 1, consisting of a satellite emulator for the generation of K satellite signals (or a user activity data signal generator [4]), which is connected to the channel emulator with a connectivity of $K \times M$. The K satellite signals are convolved with $K \times M$ different channel impulse responses including the characteristic of the propagation channel as well as the steering vector that is necessary for the wave-field synthesis (WFS). The M outputs are connected to the emulation antennas, enabling the system to reproduce the spatial characteristics of the channel. The signals are received by D antennas of the DUT. Using an anechoic chamber, the testbed can be completely separated from the outer radio environment. For an accurate emulation of the spatial structure, applying the channel emulator as described, a double directional geometry based channel model can be used.

In [5], [6], measurements-based models with high accuracy were presented, nevertheless the angular domain has been neglected or overly simplified. On the contrary, models as described in [7], [8], [9] are better suited for the proposed testbed as each individual propagation path is described by its direction of arrival (DoA), time delay of arrival (TDoA), and complex polarimetric path weight.

In this contribution, we focus on the analysis of the polar-

978-1-4799-1481-4/14/$31.00 ©2014 IEEE

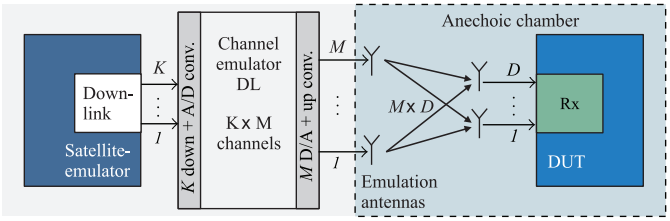

Fig. 1. Schematic of a GNSS OTA*in*VEE test-system using satellite emulator.

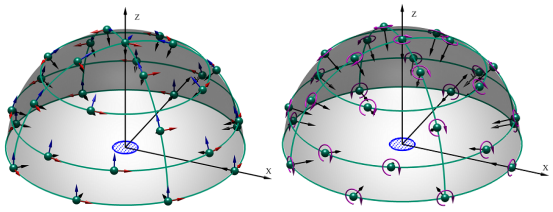

Fig. 3. Two possible emulation antenna setups. The green spheres denote the emulation antennas, while the area marked in blue is the sweet spot. The arrows describe the antenna polarization.

ization of the emulation antennas in conjunction with their geometry, to achieve the desired field quality for different polarizations of the impinging plane waves to be emulated.

The paper is organized as follows: Section II introduces the application scenario in the context of global navigation satellite systems (GNSS). Section III gives a view onto the emulation setup for the scenario emulation, followed by the WFS background in Section IV. The results are interpreted in Section V, closing with the conclusions in Section VI.

II. Scenario

For a GNSS application, relevant signals may impinge from the direction of a satellite, a jammer/spoofer, or a scatterer (cf. Figure 2, [10]). Thus, the emulation system must be able to reproduce all azimuth and elevation angles in the upper hemisphere. The simulated frequency is at f =1.575 GHz. To accommodate the typical size for a GNSS beamforming array, we design the emulation system such that the field is reproduced accurately in an area of diameter 20 cm, the so-called *sweet spot*.

We focus on circular polarized waves, which are synthesized either with dual-linear polarized emulation antennas, where both ports are fed independently, or with single-circular polarized emulation antennas (RHCP or LHCP).

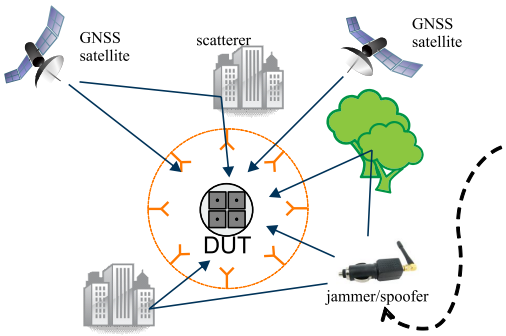

Fig. 2. Exemplary GNSS test scenario to assess the robustness against a jammer/spoofer.

III. Emulation setup

Figure 3 shows possible setups applicable for the synthesis of circular polarized wave fields. For the sake of an homogeneous quality of the wave field across all azimuth and elevation angles to be emulated, a Lebedev grid with 29 points is used (cf. [11], [12] for further details on the emulation antenna distribution). The left plot shows the use of 29 dual-linear polarized emulation antennas, where the horizontal and vertical ports can be fed independently. On the right, 29 single-circular polarized emulation antennas are used.

IV. Wave-Field Synthesis

This section briefly reviews the wave field synthesis (WFS) fundamentals, presenting the full-polarimetric extension of the previous studies in [11] and [13]. Let K denote the number of transmitting satellites. As already mentioned in the introduction, we model the propagation channel at any given time t as a sum of plane waves, such that for the k-th satellite we have Q_k paths. The q-th path is characterized by a DoA, a TDOA, and a complex polarimetric path weight, which we denote with $\Omega_{q,k}(t)$, $\tau_{q,k}(t)$, and $\boldsymbol{\gamma}_{q,k}(t)$, respectively. Note that the DoA comprises both azimuth and elevation, so that $\Omega_{q,k}(t) = \{\varphi_{q,k}(t), \vartheta_{q,k}(t)\}$.

The goal of the WFS is to generate a plane wave within the sweet spot for each of the Q_k paths for each of the K satellites as accurately as possible. To do so, we define the vector valued function $\boldsymbol{s}$ which, given a DoA and a complex polarimetric path weight, returns the complex amplitude and phase weights with which we need to feed the M emulation antennas. Expressing the output of $\boldsymbol{s}$ in frequency domain we have $\boldsymbol{s} : \{f, \Omega_{q,k}(t), \boldsymbol{\gamma}_{q,k}(t)\} \rightarrow \mathbb{C}^{M\times 1}$.

Putting the propagation model and the WFS together, we can compute the complex valued signal $\boldsymbol{y}(f,t) \in \mathbb{C}^{M\times 1}$ at time t and frequency f to be fed to the M emulation antenna ports as

$$\boldsymbol{y}(f,t) = \sum_{k=1}^{K} g_k(f,t) \cdot \sum_{q=1}^{Q_k} \left[h(f,\tau_{q,k}(t)) \cdot \boldsymbol{s}(f,\Omega_{q,k}(t),\boldsymbol{\gamma}_{q,k}(t))\right] \in \mathbb{C}^{M\times 1}, \quad (1)$$

where $g_k(f,t)$ is the radiated signal of the k-th satellite, $h(f,\tau_{q,k}(t)) = \exp(-\mathrm{j}2\pi f \tau_{q,k}(t))$ accounts for the phase shift given by the TDoA $\tau_{q,k}(t)$, and the function $\boldsymbol{s}$ acts as a *steering vector* for the array made of the emulation antennas. Note that for simplicity, we have omitted the Doppler shift. However, this can be easily included in order to consider highly mobile scenarios.

We now address the problem of finding the vector function $\boldsymbol{s}$. To do so, we define N points uniformly distributed within

the sweet spot. The number N is chosen to meet the spatial sampling theorem [11]. Let the position vector $\boldsymbol{o}_n$ denote the n-th point. Let further $\boldsymbol{e}(f, \boldsymbol{o}_n) \in \mathbb{C}^{3\times 1}$ denote the complex phasor along the three spatial dimensions (i.e., x, y, z) of the electric field at frequency f and position $\boldsymbol{o}_n$.

We now define the target electric field $\boldsymbol{e}_{\mathrm{ref}}(f, \boldsymbol{o}_n)$ as the field generated by an ideal plane wave characterized by Ω and $\boldsymbol{\gamma}$, namely the DoA and complex polarimetric path weight, respectively, at frequency f and position $\boldsymbol{o}_n$

$$\boldsymbol{e}_{\mathrm{ref}}(f, \boldsymbol{o}_n) = \left(\boldsymbol{I} - \frac{\boldsymbol{\kappa}\boldsymbol{\kappa}^{\mathrm{T}}}{\|\boldsymbol{\kappa}\|_2^2} \right) \cdot \boldsymbol{\gamma} \cdot \mathrm{e}^{-\mathrm{j}\cdot\boldsymbol{\kappa}^{\mathrm{T}}\boldsymbol{o}_n}, \tag{2}$$

where $(\cdot)^{\mathrm{T}}$ indicates transposition, $\boldsymbol{I}$ is a 3×3 identity matrix, and $\boldsymbol{\kappa}$ is the wave vector, i.e., a vector pointing in the direction of propagation having norm $2\pi f/c$, with c being the velocity.

Given a certain steering vector $\boldsymbol{s}$, the synthesized electric field $\boldsymbol{e}_{\mathrm{syn}}(f, \boldsymbol{o}_n)$ at frequency f and position $\boldsymbol{o}_n$ can be computed as $\boldsymbol{e}_{\mathrm{syn}}(f, \boldsymbol{o}_n) = \boldsymbol{X}(f, \boldsymbol{o}_n) \cdot \boldsymbol{s}$, where the transfer matrix $\boldsymbol{X}(f, \boldsymbol{o}_n) \in \mathbb{C}^{3\times M}$ accounts for the contributions to the field of each of the M antenna ports. Its m-th column, denoted by $\boldsymbol{x}_m(f, \boldsymbol{o}_n)$, can be computed as

$$\boldsymbol{x}_m(f, \boldsymbol{o}_n) = \underbrace{\left(\boldsymbol{I} - \frac{\boldsymbol{p}_{m,n}\boldsymbol{p}_{m,n}^{\mathrm{T}}}{d_{m,n}^2} \right) \boldsymbol{\alpha}_m}_{\text{polarization}} \cdot \underbrace{\rho(d_{m,n})}_{\text{magnitude}} \cdot \underbrace{\mathrm{e}^{-\mathrm{j}\frac{2\pi f}{c}\cdot d_{m,n}}}_{\text{phase}},$$

where $\boldsymbol{p}_{m,n}$ is the vector from the origin of the m-th antenna to the n-th optimization point $\boldsymbol{o}_n$ having norm $\|\boldsymbol{p}_{m,n}\|_2 = d_{m,n}$, $\boldsymbol{\alpha}_m$ is the polarization vector of the m-th antenna, and $\rho(d_{m,n})$ is the path loss term $\rho(d_{m,n}) = \lambda/(4\pi d_{m,n})$.

The vector valued function $\boldsymbol{s}$ is defined as the solution of a minimization problem, namely minimizing the quadratic error between the target field $\boldsymbol{e}_{\mathrm{ref}}(f, \boldsymbol{o}_n)$ and the synthesized field $\boldsymbol{e}_{\mathrm{syn}}(f, \boldsymbol{o}_n)$ over the N points chosen uniformly within the sweet spot

$$\boldsymbol{s}(f, \Omega, \boldsymbol{\gamma}) = \arg\min_{\boldsymbol{s}^\star} \sum_{n=1}^{N} \|\boldsymbol{e}_{\mathrm{syn}}(f, \boldsymbol{o}_n) - \boldsymbol{e}_{\mathrm{ref}}(f, \boldsymbol{o}_n)\|_2^2 \tag{3}$$

with $\boldsymbol{e}_{\mathrm{syn}}(f, \boldsymbol{o}_n) = \boldsymbol{X}(f, \boldsymbol{o}_n) \cdot \boldsymbol{s}^\star$, where the dependencies of $\boldsymbol{X}$ and $\boldsymbol{e}_{\mathrm{ref}}(f, \boldsymbol{o}_n)$ from Ω, and $\boldsymbol{\gamma}$, omitted for simplicity, can be obtained easily from the previous equations. The wave field synthesis is done for each impinging wave from the K satellites, its multiple reflections as well as the jammer and spoofer signals independently, which linearly superimpose in the emulation process.

V. Wave-Field Synthesis Quality Analysis

To assess the achievable field quality, we employ the error vector magnitude (EVM, in dB) as an independent metric. Note that this antenna-independent metric is chosen other than analyzing the DoA estimation error of an specific antenna array at a specific SNR in the emulated field, The EVM is defined as

$$\mathrm{EVM}(f, \boldsymbol{v}) = 10 \cdot \log\left(\frac{\|\boldsymbol{e}_{\mathrm{syn}}(f, \boldsymbol{v}) - \boldsymbol{e}_{\mathrm{ref}}(f, \boldsymbol{v})\|_2^2}{\|\boldsymbol{e}_{\mathrm{ref}}(f, \boldsymbol{v})\|_2^2} \right),$$

where the $\mathrm{EVM}(f, \boldsymbol{v})$ is calculated for an arbitrary position $\boldsymbol{v}$. In the following, we define the mean EVM as the average over W points $\boldsymbol{v}$ equidistantly distributed in the sweet spot and fulfilling the spatial sampling theorem. In this way the EVM specifies above which SNR an antenna array would experience a different field than in reality resulting in a bias for all signal processing algorithms in the receiver.

Figure 4 shows a comparison of the WFS quality between using dual-linear polarized (both ports are fed independently) and circular polarized emulation antennas (only one port per antenna) for synthesizing a circular polarized wave (RHCP) from an elevation angle of 90°. The top plots show the EVM values in and outside the sweet spot. The achieved quality is almost the same for both antenna setups. The bottom plot is depicting the magnitudes of the elements of the steering vector $\boldsymbol{s}$. We plotted the magnitude of the elements of the vector $\boldsymbol{s}$ for the dual-linear (H&V) vs. the single-circular polarized case in the same plot for comparison. The top view of the emulation antennas is given in the upper right corner of the bar plot. The impinging wave is marked with a green circle.

Looking at emulation antenna $m = 5$, we see the biggest contribution in terms of power to the resulting wave, as the antenna and the impinging wave direction are co-located. The contribution of the adjacent emulation antennas decrease as the angular distance increases. Each group of four emulation antennas (18–21, 14–17, ...) have identical magnitudes because of the symmetry of the problem.

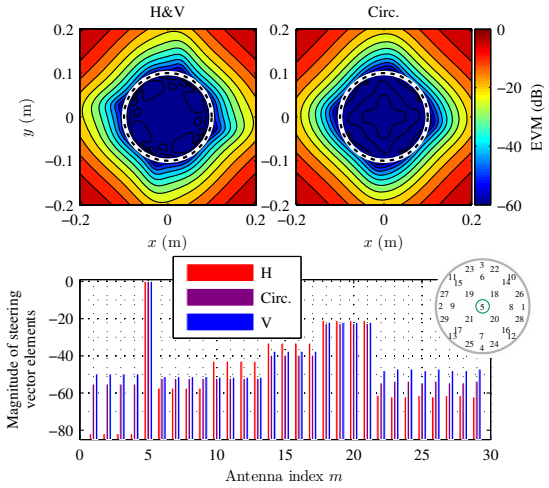

Fig. 4. Synthesis of a circular polarized plane wave from 90° elevation. The top plots show the resulting EVM. The bottom plot shows the antenna excitation for the m-th antenna. The green circle shows the direction of the impinging wave. Mean EVM for the dual-linear polarized case (H&V) is -63.7 dB, -61.9 dB for single-circular polarized case (Circ).

Considering all possible angles for a single impinging plane wave, Figure 5 depicts the field quality for the dual-linear polarized case (left) and for the single-circular polarized one (right). The color represents the mean EVM inside the sweet spot for the corresponding impinging angle. It can be seen that the mean EVM, comparing the dual-linear polarized and the single-circular polarized case is almost identical when

the impinging wave direction is placed close to an emulation antenna position (cf. Figure 4). For the other directions, when the impinging wave direction is displaced from an emulation antenna position, we can see a drop of synthesis quality between 4.7 dB and 4.9 dB. Comparing the dual-linear and single-circular polarized case and keeping in mind that a channel emulator with two times the number of outputs is needed for the dual-linear polarized case (58 instead of 29 antenna ports), the benefit in synthesis quality due to the larger number of fed emulation antennas is rather small (4.7 dB on average).

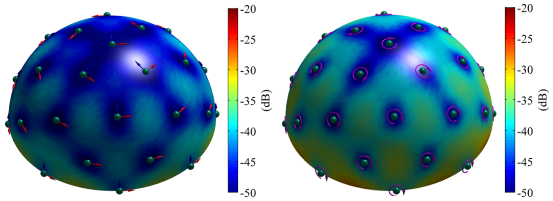

Fig. 5. Synthesis of a circular polarized wave with: 29 dual-linear polarized emulation antennas (left, $\mathrm{EVM_{max}}$=-33.7 dB, $\mathrm{EVM_{avg}}$=-42.8 dB), and with 29 single-circular polarized emulation antennas (right, $\mathrm{EVM_{max}}$=-28.8 dB, $\mathrm{EVM_{avg}}$=-38.1 dB). The colors denote the mean EVM w.r.t. the direction the impinging wave.

Please note that in the case of using dual-circular polarized emulation antennas (not shown here), we achieve an identical field quality compared to the dual-linear case, as both configurations can reproduce the very same polarization states.

When the system is implemented, the transfer matrix $\boldsymbol{X}$ as well as occurring imperfections (e. g. the emulation antenna positioning) will be considered through the calibration measurement process using a positioner and EM-probes for each of the three spatial dimensions. This means the antennas can be placed as accurate as possible but the remaining positioning inaccuracies will not result in a degradation of the emulated field quality due to the calibration.

VI. Conclusion

This contribution analyzed the feasibility of 3D wave-field synthesis to emulate global navigation satellite system scenarios in a virtual electromagnetic environment. Different emulation antenna setups for 3D WFS were investigated, comparing a dual-linear polarized emulation antenna setup with a single-circular polarized one. It could be shown that an overall accuracy (for impinging waves of arbitrary direction) better than 30 dB can be achieved.

Analyzing the mean EVM for all setups and arbitrary directions of the impinging wave, it can be seen that the mean EVM is -28.8 dB at maximum. With this results and keeping in mind that satellite navigation receivers do not operate at SNRs larger than 30 dB (already after correlation) the synthesized field quality is sufficient for most GNSS test cases. For the case that only RHCP waves are impinging, the single-circular polarized antenna setup can be chosen with the advantage of less hardware effort (number of channels of the channel emulator). However, for scenarios with arbitrary polarization of the impinging waves the dual-linear or dual-circular polarized emulation antenna setup is mandatory to achieve a sufficient field quality.

It was shown that a further reduction of hardware complexity by means of the number of radiating emulation antennas (equal to the required number of outputs of a channel emulator) can be achieved choosing the single-circular polarized emulation antenna setup with tolerable error. The results presented in this contribution indicate that 3D WFS for GNSS testing under controlled, realistic and repeatable conditions will become a reality in the near future.

Acknowledgment

This work has been performed within the International Graduate School on Mobile Communications (MobicoM). It is supported by the German Research Foundation DFG (GRK 1487) and the Carl Zeiss Foundation.

References

[1] M. Rumney, R. Pirkl, M. H. Landmann, and D. A. Sanchez-Hernandez, "MIMO over-the-air research, development, and testing," *International Journal of Antennas and Propagation*, vol. 2012, 2012.

[2] Y. Jing, Z. Wen, H. Kong, S. Duffy, and M. Rumney, "Two-stage over the air (OTA) test method for MIMO device performance evaluation," in *Antennas and Propagation (APSURSI), 2011 IEEE International Symposium on*, July 2011, pp. 71–74.

[3] R. K. Sharma, W. Kotterman, M. H. Landmann, C. Schirmer, C. Schneider, F. Wollenschläger, G. Del Galdo, M. Hein, and R. S. Thomä, "Over-the-air testing of cognitive radio nodes in a virtual electromagnetic environment," *International Journal of Antennas and Propagation*, vol. 2013, 2013.

[4] C. Schirmer, M. Alsharef, W. Kotterman, A. Ihlow, G. Del Galdo, and A. Heuberger, "High time resolution spectrum occupancy model for testing of cognitive radio devices," in *24th IEEE International Symposium on Personal, Indoor and Mobile Radio Communications (PIMRC)*, 2013.

[5] A. Steingass and A. Lehner, "Measuring the navigation multipath channel – a statistical analysis," in *Proceedings of the 17th International Technical Meeting of the Satellite Division of The Institute of Navigation (ION GNSS 2004)*, 2004, pp. 1157 – 1164.

[6] A. Lehner and E. Steingass, "A novel channel model for land mobile satellite navigation," in *Institute of Navigation Conference ION GNSS 2005*, pp. 13–16.

[7] S. Jaeckel, K. Borner, L. Thiele, and V. Jungnickel, "A geometric polarization rotation model for the 3-d spatial channel model," *Antennas and Propagation, IEEE Transactions on*, vol. 60, no. 12, pp. 5966–5977, Dec 2012.

[8] E. Eberlein, F. Burkhardt, S. G., S. Jaeckel, and R. Prieto-Cerdeira, "MIMOSA analysis of the MIMO channel for LMS systems," in *Space Communications*, 2013, pp. 145–158.

[9] C. Schneider, M. Narandzic, M. Kaske, G. Sommerkorn, and R. Thomä, "Large scale parameter for the winner ii channel model at 2.53 ghz in urban macro cell," in *Vehicular Technology Conference (VTC 2010-Spring), 2010 IEEE 71st*, May 2010, pp. 1–5.

[10] A. Rügamer, G. Del Galdo, J. Mahr, G. Rohmer, G. Siegert, and M. Landmann, "GNSS Over-the-Air Testing using Wave Field Synthesis," in *in Proceedings of the 26th International Technical Meeting of the Satellite Division of the Insitute of Navigation, ION GNSS+ 2013, September 16-20, 2013, Nashville, Tennessee, USA*, September 2013.

[11] C. Schirmer, M. H. Landmann, W. A. T. Kotterman, M. Hein, R. S. Thomä, G. Del Galdo, and A. Heuberger, "3D wave-field synthesis for testing of radio devices," in *8th European Conference on Antennas and Propagation*, 2014, accepted.

[12] W. A. T. Kotterman, C. Schirmer, M. H. Landmann, and G. Del Galdo, "On arranging dual-polarised antennas in 3D wave field synthesis," in *8th European Conference on Antennas and Propagation*, 2014, accepted.

[13] P. Kyösti, T. Jämsä, and J.-P. Nuutinen, "Channel modelling for multi-probe Over-the-Air MIMO testing," *International Journal of Antennas and Propagation*, vol. 2012, 2012.